Journal of Hazardous Materials 489 (2025) 137647

Contents lists available at ScienceDirect

Journal of Hazardous Materials

journal homepage: www.elsevier.com/locate/jhazmat

Cellular internalization pathways of environmentally exposed microplastic particles: Phagocytosis or macropinocytosis?

Anja F.R.M. Ramsperger [a,b,1], Simon Wieland [a,b,1], Magdalena V. Wilde [c,d,1], Thomas Fröhlich [c], Holger Kress [b,2], Christian Laforsch [a,*,2]

[a] Animal Ecology I and BayCEER, University of Bayreuth, Bayreuth, Germany
[b] Biological Physics, University of Bayreuth, Bayreuth, Germany
[c] Gene Center Munich, Laboratory for Functional Genome Analysis (LAFUGA), LMU München, Munich, Germany
[d] Department of Earth and Environmental Sciences, Paleontology & Geobiology, LMU München, Munich, Germany

HIGHLIGHTS

- Cellular internalization pathways for MP differ depending on eco-corona origin.
- Ecocorona from different environments differ in their protein composition.
- Freshwater microplastics become internalized by maropinocytosis and phagocytosis.
- Saltwater microplastics become internalized mainly via macropinocytosis.

GRAPHICAL ABSTRACT

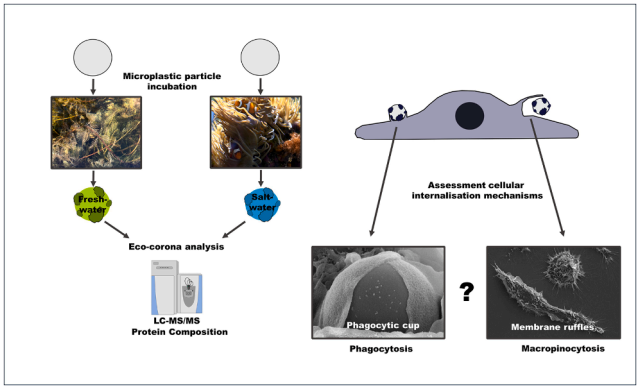

ARTICLE INFO

Keywords:
Microplastics
Eco-corona
Microfluidics
Cellular internalization
Phagocytosis
Macropinocytosis
Proteomics
Optical tweezers

ABSTRACT

Microplastic particles (MP) ubiquitously occur in all environmental compartments where they interact with biomolecules, forming an eco-corona on their surfaces. The eco-corona affects the surface properties of MP and consequently how they interact with cells. Proteins, an integral component within the eco-corona, may serve as a ligand driving the interaction of MP with membrane receptors. To date, it is not known, whether eco-coronae originating from different environmental media differ in their proteinaceous compositions and whether these particles interact differently with cells. We show that the protein composition of the eco-coronae formed in freshwater (FW) and salt water (SW) are distinct from each other. We did not observe different adhesion strengths between MP coated with different eco-coronae and cells. However, the internalization efficiency and the underlying internalization mechanisms significantly differed between FW- and SW eco-coronae. By inhibiting actin-driven and receptor-mediated internalization processes using Cytochalasin-D, Amiloride, and Amantadine,

* Corresponding author.
E-mail address: christian.laforsch@uni-bayreuth.de (C. Laforsch).
[1] shared first authorship
[2] shared senior authorship

https://doi.org/10.1016/j.jhazmat.2025.137647
Received 5 November 2024; Received in revised form 24 January 2025; Accepted 15 February 2025
Available online 17 February 2025

we show that FW microplastic particles predominantly become internalized via phagocytosis, while macropinocytosis is more important for SW microplastic particles. Overall, our findings show that the origin of eco-coronae coatings are important factors for the cellular internalization of microplastic particles. This highlights the relevance of eco-coronae for adverse effects of environmentally relevant microplastic particles on cells and organisms.

1. Introduction

Microplastic particles, synthetic polymeric particles smaller than 1 mm [1], are ubiquitously found in all environmental compartments [2]. The overall abundance of microplastic particles comes along with the potential risk of particle uptake by organisms, including humans. To date, numerous studies are showing the uptake of microplastic particles by various organisms ranging from invertebrates such as zooplankton [3–5] and mussels [6,7] up to vertebrates [8]. One risk associated with the uptake of microplastic particles that has been intensively discussed is the translocation of microplastic particles from the primarily exposed organs, like the gastrointestinal or respiratory tract, into other tissues [9,10]. The translocation of microplastic particles into tissues was suggested to occur via cellular internalization and subsequent particle transportation [9–11]. Once a cell encounters foreign particulate matter in the micrometre-size range, a potential internalization can be subdivided into two steps. Within the first step, the surface of the particle interacts with the cell either by binding to cellular receptors [12,13] or by unspecific (e.g. electrostatic) interactions with the cell membrane [14]. Subsequently, the particle can be internalized by various mechanisms. Among these mechanisms for endocytosis, the actin-dependent processes phagocytosis and macropinocytosis are the ones which are relevant for micron-sized particles [15–17]. Phagocytosis is initiated by the interaction of ligands on the surface of a particle with specific receptors on the cellular membrane [13,17,18], whereas macropinocytosis can either be performed constitutively for nutrient acquisition in cells of the innate immune system or can be induced by growth factors [18].

Whether or not microplastic particles interact with a cell depends on the particles surface properties, such as the zeta potential or surface coatings [19–21].

Microplastic particles in the environment exhibit surface modifications, a so called eco-corona formation, compared to their pristine counterparts which are often used in effect studies [22]. Most of the findings on the formation of coronas on particle surfaces originate from nanomaterial sciences. Those studies mainly used artificial media such as blood or serum from a single organism [23–26], or specific culture media [27,29]. It was described that within less than half a minute, the first proteins attach to a particle surface, and the amount of proteins was described to increase with increasing incubation time [26]. With time, a hard corona develops, consisting of proteins with high binding affinities. On top of the hard corona, loosely bound proteins develop a soft corona [23,31]. Although the whole protein corona, the hard and the soft corona, is not a static but highly dynamic system, initial bound proteins forming the hard corona stay as a fingerprint of the coronas' history even after the particle enters a different compartment [24]. Once a particle is released into the environment, the surrounding media is much more complex than in experimental setups using well-defined media. It hosts different organisms, conditioning the media with specific metabolites [33]. As a result, a particle released into this environment faces a plethora of different biomolecules [33], consequently coating the particle with an eco-corona [35,37,39,41]. Wheeler et al. [43] highlighted in their comprehensive review that the molecular diversity of the eco-corona reflects the biodiversity of the environment in which it is formed. The often unknown biomolecules occurring within the environmental media make identifying the constituents of the eco-corona challenging. So far, the components of an eco-corona were described as proteins, humic and fulvic acids, amino acids, lipids, polysaccharides, and carbohydrates [41,45,47], which change the particles' physico-chemical surface properties. Although proteins do not necessarily compose the highest share of biomolecules within an eco-corona, the robust body of literature on proteins allows the characterization and increases insights into eco-corona formation [43].

Proteins are large molecules consisting of different combinations of amino acids and can function as structural components, transport and storage, messengers, enzymes and antibodies [28]. They are released during the metabolisms of organisms into their surrounding environment, and consequently adsorb and accumulate on any available surface [30]. Here, depending on the organisms present in an ecosystem the released proteins can be different and consequently can lead to different protein composition of the eco-corona. In general, the coating with an eco-corona changes the biological identity of a particle by introducing a soft layer onto the particles making them softer [32], and changes the microplastic particles' zeta potential, which can induce a modified interaction to cellular membranes, biodistribution, immunological responses and toxicity [52] compared to microplastic particles without an eco-corona [19]. In the case of a stronger attachment of the particles to cells, the internalization into the cells can be enhanced [19,21]. The attachment of such microplastic particles with a cellular membrane can either be mediated by unspecific electrostatic forces or by the specific interaction of the components of the eco-corona with receptors of the cell membrane. Here, especially proteins, can serve as a ligand for receptor binding.

In our study we characterized the proteinaceous composition of two different eco-coronae, fresh- (FW) and salt water (SW) with liquid chromatography-tandem mass spectrometry (LC-MS/MS). Furthermore, we assessed whether different eco-coronae lead to differences in particle-cell interactions and characterized their binding probability and adhesion forces to cellular membranes compared to microplastic particles without an eco-corona. Additionally, we analysed the internalisation efficiency and investigated whether there are differences in the internalization mechanisms of microplastic particles coated with different eco-coronae, by inhibiting either phagocytosis or macropinocytosis.

2. Materials & methods

2.1. Microplastic particle characterization

2.1.1. Microplastic particles and pre-treatment conditions

Plain, non-fluorescent, white monodisperse polystyrene spheres with a diameter of 3 μm (MICROMOD, Rostock, Germany, white particles, micromer® plain, Prod.-Nr.: 01–00–303) were used as microplastic particles. The particles were exposed to the corresponding environmental media as described in Ramsperger et al. [21]. In brief, the microplastic particles were incubated for two weeks in FW or SW to obtain an eco-corona or in ultrapure water (UW), serving as control particles without an eco-corona (Veolia pure lab flex, Veolia, Celle, Germany, and Milli-Q, MERCK MILLIPORE, Darmstadt, Germany). The freshwater was obtained from a controlled mesocosm facility at the University of Bayreuth and the saltwater originates from a highly diverse populated seawater aquarium at the Department of Animal Ecology I, University of Bayreuth. 100 μL of microplastic particle stock solution (50 mg mL^{-1}) was added to 900 μL of the corresponding water sample (FW, SW, UW) in a glass vial (autosampler vials, 1.2 mL, neoLab, Heidelberg, Germany). To ensure vital microbial communities, the

water in the FW and SW samples was changed three times per week. To do so the samples were centrifuged (2000 × g, 20 min, room temperature), and 900 μL of supernatant was replaced by the same amount of new corresponding water. The same procedure was performed for the UW treatment. Before adding the UW, it was filtered (Whatman Puradisc syringe filter, 0.2 μm, GE Healthcare, Freiburg, Germany) under sterile conditions. To prevent aggregation of the microplastic particles by sedimentation, all samples were placed on a shaker (100 round per min (rpm) at room temperature). Although we did not add surfactant to avoid aggregation of the microplastic particles, only occasionally aggregates were found in all samples. Furthermore, particles were opsonized with immunoglobulin G (IgG) to serve as a positive control treatment for phagocytosis. Therefore antibodies (native immunoglobulin G primary antibodies from mouse serum MERCK MILLIPORE, Darmstadt, Germany) were passively adsorbed onto carboxylated microplastic particles (MICROMOD, Rostock, Germany, white particles, micromer® COOH, Prod.-Nr.: 01–02–303) as described previously [34, 36,38]. Opsonization was verified by antibody-antibody labelling with goat anti-Mouse IgG cross-adsorbed fluorescent secondary antibody (Dy-Light 488, THERMO SCIENTIFIC). The concentration of all microplastic particles samples was determined using a haemocytometer (Neubauer improved, Brand, Wertheim, Germany) to ensure comparable particle concentrations.

2.1.2. Surface structure of the microplastic particles

Microplastic particles of all treatments were pipetted onto a silicon wafer and fixed using Karnovsky's fixative (2 % paraformaldehyde (PFA) (reagent grade, Sigma Aldrich, Merck KgA, Germany) and 2.5 % glutaraldehyde (for electron microscopy, Carl Roth GmbH, Germany) in 1 × phosphate buffer saline (PBS)) prior to dehydration in an ethanol series (30 %, 50 %, 70 %, 80 %, 90 % for 30 min each, 95 % and absolute ethanol for 1 h each, Ethanol purity >99.9 %, VWR International S.A.S., France) and dried in hexamethyldisilazane (HMDS, purity > 98 %, Carl Roth GmbH, Germany) [40]. The silicon wafers were mounted on carbon conductive tabs (Ø 12 mm Plano GmbH, Wetzlar, Germany) fixed to aluminum stubs (Ø 12 mm, Plano GmbH, Wetzlar, Germany). The stubs were then transferred into a desiccator and stored until the images were acquired. Samples were subsequently coated with a 4 nm-thick platinum layer (208HR sputter coaressington, Watford, UK) and analyzed using a Scanning Electron Microscope (SEM, FEI Apreo Volumescope, Thermo Fisher Scientific, magnification 5000–6500, 5 kV, Everhart-Thornley detector).

2.1.3. Proteinaceous composition of the eco-corona

For proteome analysis, 500 μL of incubated microplastic particles were centrifuged for 15 min (4°C, 500 x g). Supernatant was removed and 50 μL of 2x Laemmli buffer (0.25 M Tris-HCL; pH 6.8, 40 % (v/v) Glycerol, 8 % (v/v) SDS, 0.4 % (v/v) 1 % bromphenol blue) were added to the particles, vortexed shortly, incubated at 95°C (5 min) and centrifuged for 5 min (20,000 x g). Samples were then transferred onto a NuPAGE 4–12 % Bis-Tris Gel (Invitrogen, USA). Gels were run for 4 min at 200 V and subsequently stained overnight using Roti Blue staining solution (Roth, Germany). Protein-containing areas were excised, destained and washed with 50 mM NH_4HCO_3. Supernatant was discarded, samples were reduced with 45 mM DTE (30 min, 55°C) and subsequently alkylated with 100 mM iodoacetamide in the dark at room temperature. Gel pieces were washed, and a sequential in-gel digestion was performed using Lys-C (4 h, 37°C, Lysyl Endopeptidase, Mass Spectrometry Grade (FUJIFILM Wako Pure Chemical Corporation, USA)) followed by trypsin (17 h, 37°C, 200 ng trypsin (sequencing grade modified trypsin, Promega, Germany)). Supernatants were collected, and peptides were extracted using 70 % acetonitrile (ACN). Collected supernatants were pooled and dried using a vacuum centrifuge (Vacuum concentrator, Bachofer, Germany).

Samples were dissolved in 15 μL solvent A (0.1 % formic acid), loaded on a trap column (PEP-Map100 C18, 75 μm x 2 cm, 3 μm particles (Thermo Fisher Scientific, U.S.A)) and separated on a reversed-phase column (PepMap RSLC C18, 75 μm × 50 cm, 2 μm particles, Thermo Scientific, U.S.A) at a flow rate of 250 nL/min with a 30 min gradient of 3–25 % solvent B followed by 5 min increase to 40 %. Solvent B consisted of 0.1 % formic acid in ACN. After separation, the column was washed with 85 % solvent B for 10 min. MS/MS analysis was performed with a Q Exactive HF-X mass spectrometer (Thermo Scientific, U.S.A). The data-dependent acquisition method consisted of cycles of one MS scan with a mass range of m/z 300–1600 at a resolution of 60,000, followed by a maximum of 15 MS/MS scans at a resolution of 15,000.

Spectra were searched with MASCOT V2.6.2 (Matrix Science Limited, UK) [42]. The MS/MS data was searched against two different databases. In one case we used a bacteria subset of the National Center for Biotechnology Information protein (NCBIprot) database (updated: Nov 2020), in the other a compiled algae database downloaded from NCBI (March 2022). In both cases an additional common contaminant database (from MaxQuant) was used. An emPAI quantification [44] was done in Scaffold (version Scaffold_4.10.0, Proteome Software Inc., Portland, USA) and only proteins with a protein identification rate higher than 95 % were further analyzed. The mass spectrometry proteomics data have been deposited to the ProteomeXchange Consortium (http://proteomecentral.proteomexchange.org) via the PRIDE partner repository with the dataset identifier PXD050078 [46].

For protein quantity estimations, all peaks in the total ion chromatogram (TIC) were integrated and areas calculated using the Xcalibur Qual Browser (Thermo Fisher Scientific, U.S.A). Total areas were corrected by subtracting the peak areas of a blank run without sample. The ratios between protein amounts from the IgG preparation and the samples were calculated.

2.2. Cell experiments

2.2.1. Cell line and cell culture conditions

Murine macrophage J774A.1 cells (DSMZ, Braunschweig, Germany) were cultured as described previously [19,21,36]. In brief, cells were cultured in Dulbecco's Modified Eagle's Medium (DMEM, Lonza Group Ltd, Basel, Switzerland), supplemented with 10 % v/v FCS (Sigma Aldrich, St. Louis, USA) and 100 U/mL penicillin/streptomycin (Lonza Group Ltd, Basel, Switzerland) in T-25 culture flasks (CORNING, New York, USA) under standard cell culture conditions (37 °C, 5 % CO2, humidified) and passaged three times per week. Before the experiments, the cells were scraped off, centrifuged (200 × g, 2 min) and resuspended with 5 mL cell culture media.

2.2.2. Adhesion forces of microplastic particles to cells

To quantify the adhesion forces of microplastic particles to cells, we performed experiments using a microfluidic microscopy platform (described in supplementary information and Wieland *et al.* [19]) and optical tweezers. The optical tweezers setup was based on the optical tweezers kit provided by Thorlabs (Modular Optical Tweezers, OTKB/M, Thorlabs GmbH, Bergkirchen, Germany) together with a backfocal plane detection module (OTKBFM, Thorlabs GmbH, Bergkirchen, Germany) to enable quantitative force measurements. The microscope's beam path was illuminated using a white LED (LEDWE-15, Thorlabs GmbH, Bergkirchen, Germany). The visible light of the LED passed through a dichroic mirror (DMSP805, Thorlabs GmbH, Bergkirchen, Germany) and was focused into the sample with a condenser objective (Nikon E Plan, 10 x, NA 0.25). The sample was observed using a 100 × oil immersion objective (Nikon E Plan, 100 x, NA 1.25). The visible light passed a second dichroic mirror (DMSP805, Thorlabs GmbH, Bergkirchen, Germany) and was focused on a CMOS camera (DCC1240C, Thorlabs GmbH, Bergkirchen, Germany) using an achromatic tube lens with 200 mm focal length (AC254–200-A, Thorlabs GmbH, Bergkirchen, Germany). To generate the optical trap, a 975 nm diode laser (BL976-PAG500, Thorlabs GmbH, Bergkirchen, Germany) together with a laser diode controller (LDC 210 C, Thorlabs GmbH, Bergkirchen,

Germany) and a temperature controller (TED 200 C, Thorlabs GmbH, Bergkirchen, Germany) was used. The laser beam was collimated using a FiberPort (PAF-X-7-B, Thorlabs GmbH, Bergkirchen, Germany), and expanded by a factor of 3 using a Galilean beam expander (two achromatic doublets with −50 mm (ACN254–050-B) and 150 mm (AC254–150-B) focal length, Thorlabs GmbH, Bergkirchen, Germany). The laser beam was reflected by the second dichroic mirror of the microscope's beam path and coupled into the objective, which focused the laser beam in the sample to generate the optical trap. After the laser beam passed through the sample, it was collected by the condenser objective. It was then reflected by the first dichroic mirror of the microscope's beam path into the backfocal plane detection module. The laser beam was focused by a 40 mm lens (LB1027-B, Thorlabs GmbH, Bergkirchen, Germany) and weakened by an absorptive filter (OD 0.6, NE06B, Thorlabs GmbH, Bergkirchen, Germany). The focused laser beam was then detected using a quadrant photodiode (QPD, PDQ80A, Thorlabs GmbH, Bergkirchen, Germany), enabling to measure slight shifts in the beam position, which correspond to shifts in the position of the trapped particle. The sample was placed into the light path using a piezo stage (MAX311D/M, Thorlabs GmbH, Bergkirchen, Germany) that was controlled using three T-Cube piezo drivers (TPZ001, Thorlabs GmbH, Bergkirchen, Germany), enabling a precise positioning in *x*-, *y*-, and z-direction. Together with strain gauge readers (TSG001, Thorlabs GmbH, Bergkirchen, Germany) for the *x*- and *y*-direction, precise automatic positioning of the sample with a resolution of up to 5 nm was possible.

To perform the adhesion experiments, the cells were counted using a haemocytometer (Neubauer improved, Brand, Wertheim, Germany) and 50,000 cells were seeded on glass coverslips (diameter: 18 mm, #1, MENZEL GLAESER, Braunschweig, Germany) in 12-well plates (CellStar, GREINER BIO-ONE, Frickenhausen, Germany) in 1 mL of cell culture medium and allowed to adhere onto the coverslips under standard cell culture conditions (37 °C, 5 % CO2, humidified) overnight. Right before the experiment, the coverslips with the adherent cells were mounted to a custom-built aluminum sample holder, 84 μL of imaging medium containing approximately 10^5 microplastic particles of the respective treatment (FW, SW, UW) were added, and the sample was covered with another coverslip. Then, the sample was mounted on the optical tweezers setup.

To trap a single microplastic particle, the laser was turned on with an output power of ~150 mW. After a particle has been trapped, it was positioned next to a cell, and the trap stiffness was calibrated using the QPD to track the thermal fluctuations of the particle in the trap. The QPD signal was recorded for 6 s with a frequency of 50 kHz. From the QPD signal, the trap stiffness was calculated harnessing the powerspectral density [48]. The trap stiffness typically was 15–20 pN μm^{-1}. Each microplastic particle was calibrated individually to account for slight variations in the diameter and refractive index of the particles.

After the trap stiffness has been calibrated, a measurement was started. With the piezo stage, the cell was slowly moved towards the trapped microplastic particle, until it made contact with the cell. The contact was monitored using the QPD, and the movement of the stage was stopped after the QPD signal was set off 0.15 V (corresponds to a displacement of the particle from the trap center of approximately 30 nm). The particle-cell contact was continued for 1 s or 10 s, respectively. Then, the cell was retracted and moved to its original position to rupture the particle off the cell. This process was recorded with a framerate of 30 fps using the CMOS camera. In the video, the microplastic particle position was tracked using a cross-correlation tracker [34,36,49] to measure the displacement of the particle from the trap during the rupture phase. From the particle displacement, the adhesive force was calculated with the calibrated trap stiffness. For each particle, 10 particle-cell contacts were evaluated. Additionally, for each particle the force heterogeneity was calculated, which was defined as the maximal adhesion force measured for a particle divided by the corresponding minimal force.

2.2.3. Quantification of particle-cell-interactions, internalization and the inhibition of the internalization mechanisms

The cells from the stock culture were counted using a haemocytometer (Neubauer improved, Brand, Wertheim, Germany) and 50,000 cells were seeded on glass coverslips (diameter: 18 mm, #1, MENZEL GLAESER, Braunschweig, Germany) in 12-well plates (CellStar, GREINER BIO-ONE, Frickenhausen, Germany) in 1 mL of cell culture medium and allowed to adhere onto the coverslips under standard cell culture conditions (37 °C, 5 % CO2, humidified) overnight.

To quantify the particle-cell-interactions and internalization as well as the underlying internalization mechanisms for microplastic particles the cell culture medium was either replaced by pure cell culture medium (control treatment) or replaced by cell culture medium containing the respective inhibitor (Cytochalasin D, Amiloride or Amantadine). The concentrations of the inhibitors were chosen as described in the literature: Cytochalasin D (2 μM, diluted in DMEM) and Amiloride (130 μM, diluted in DMEM) were used to inhibit actin-dependent endocytosis in general [36,50,51,53] and Amantadine (100 μM, diluted in DMEM) was used to inhibit receptor-mediated endocytosis, in this specific case phagocytosis [54,55].

The cells treated with the corresponding inhibitor and the control cells without inhibitor were incubated for 30 min under cell culture conditions. Then, 150,000 microplastic particles pre-treated with fresh-, salt- or ultrapure water or IgG-opsonized microplastic particles were added. The cells were placed on ice for one hour to reduce cell metabolism during the particle sedimentation. Three coverslips for each microplastic particle treatment and inhibitor/control treatment combination were prepared, yielding a total of 3x4x4 = 48 coverslips. After one hour of microplastic particle sedimentation, the well plates were incubated under cell culture conditions for two hours to allow cellular internalization of the particles. Then, the cells were fixed with 4 % PFA (SIGMA-ALDRICH, St. Louis, Missouri) for 20 min on ice and subsequently labelled with Alexa Fluor Phalloidin 488 (Invitrogen, Carlsbad, USA) and dilution buffer, consisting of 98.7 % PBS, including 0.3 % Triton and 1 % bovine serum albumin (BSA, APPLICHEM, Darmstadt, Germany) to a final concentration of 1: 25 for 25 min.

To quantify the particle-cell-interactions, the procedure described in Ramsperger et al. [21] was used. In brief, to determine the total number of particle-cell-interactions on each coverslip, five randomly chosen regions of interest (ROIs, 0.10 mm^2) were selected and imaged by using a DMI 6000 microscope (LEICA, Wetzlar, Germany, HCX PL APO 63 ×/1.30 oil objective) including a spinning disc unit (CSU-X1, YOKOGAWA, Musashino, Japan) with an EMCCD camera (Evolve 512, PHOTOMETRICS, Tucson, Arizona, including an additional 1.2 × magnification lens). A differential interference contrast (DIC) microscopy image was acquired to quantify the particle-cell-interactions within the ROIs using the Fiji ImageJ cell counter software. Additionally, confocal stacks of fluorescently labelled cells were acquired using a 488 nm laser (50 mW, Sapphire 488, COHERENT, Santa Clara, California) at a spinning disc speed of 5000 rpm to excite fluorescence. Axial stacks of the cells were acquired with a vertical distance of 0.2 μm, which is sufficient to oversample the image given the axial resolution of the microscope [56]. The confocal stacks were used to calculate the area covered by cells within an ROI. The area covered by cells was detected using both the DIC and the fluorescence channel simultaneously to obtain robust results. To allow comparability between the treatments, the same number of cells were seeded for all treatments and the same number of particles were added into each sample well, as described above.

From the same samples, we visually screened each coverslip for single particle-cell-interactions to distinguish between particles that were only attached to cells and particles that were completely internalized. The same DMI 6000 microscope, including a spinning disc unit with a higher magnification (100 ×/1.40 oil objective), was used. Beginning from a randomly defined starting point, the coverslips were screened in the DIC-channel until 100–110 particle-cell-interactions

were detected, or the whole coverslip was screened entirely. Once a particle-cell-interaction was found, a DIC-image was taken, and axial stacks of fluorescently labelled cells were acquired using a 488 nm laser (50 mW, Sapphire 488, COHERENT, Santa Clara, California) at a spinning disc speed of 5000 rpm to excite fluorescence (vertical distance of the axial stacks: 0.2 μm). To evaluate the internalization of the microplastic particles, each confocal stack of cells with labelled actin filaments was analyzed with Fiji ImageJ (version: 2.0.0-rc-54/1.51 h 2016–09–08) orthogonal views. The microplastic particles used in the experiments were not fluorescent and were not directly visible in the confocal stacks. DIC images were used to mark the particle positions (using the ROI manager in Fiji ImageJ). These positions were then transferred to the confocal stacks, in which internalized particles were visible as spherical black regions within the actin network. Only microplastic particles that were entirely surrounded by actin filaments were considered to be internalized. Microplastic particles that were only partly surrounded were considered to be attached to cell membranes (Fig. 1 A and B).

2.2.4. Combination and standardization of the results

The number of particle-cell-interactions was extrapolated to the whole area of each coverslip (245.50 mm^2). As the areas on the coverslips covered by cells differ slightly between replicates and treatment-inhibitor-combinations each coverslip was standardized as described in Ramsperger et al. [21].

2.2.5. Scanning electron microscopy - cells

100,000 cells per mL were seeded one day before the experiment, and on the following day, 106 microplastic particles (10 particles per cell) of the corresponding treatment (FW or SW) were added and left to settle for one hour in ice. Afterward, the cells were transferred to cell culture conditions for two hours to allow internalization. Subsequently, the cells were fixed using Karnovsky's reagent (12 % v/v paraformaldehyde, 8 % v/v glutaraldehyde in 0.1 M buffer) for 1 h at room temperature. Cells were washed three times with ultrapure water and afterward dehydrated using an ethanol series 30 % (3 ×15 min at 4 °C), 50 % (3 ×15 min at 4 °C), 70 % (3 ×15 min at −20 °C) for 90 % (3 ×15 min at −20 °C), absolute ethanol (3 ×20 min at – 20 °C) and Hexamethyldisilazane (2 ×10 min at room temperature) and let dry overnight in a desiccator. The air-dried samples were sputtered with 2 nm platinum, and microscopy was performed using SEM (FEI Apreo Volumescope, Thermo Fisher Scientific, magnification 5000–6500,

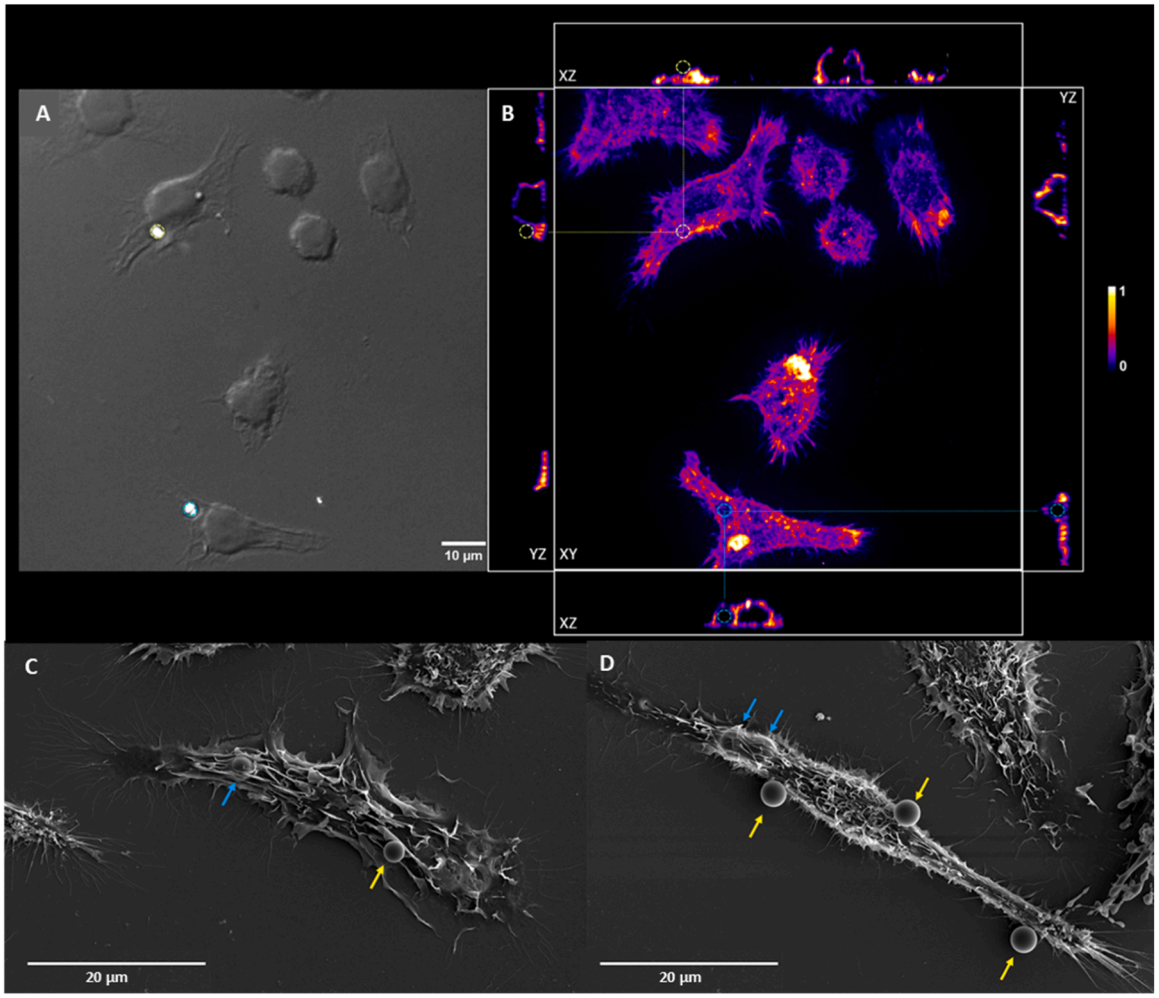

Fig. 1. Illustration of the differentiation between particles that are attached to the cells and particles that are internalized by cells. (A) Example of J77A.1 murine macrophage cells with microplastic particles incubated in SW. The DIC images were used to localize microplastic particles within the DIC images (A) and within the confocal z-stacks (B). The filamentous actin was fluorescently labeled and orthogonal views (XY-, XZ- and YZ-plane) allowed the differentiation between microplastic particles that are attached (yellow circle) to the cells and microplastic particles that are internalized (blue circle) by cells. Internalized particles are completely surrounded by filamentous actin. (C, D) Scanning electron microscopy images of J774A.1 murine macrophages incubated with 3 μm sized microplastic particles coated with an eco-corona from FW (C) and SW (D). Yellow arrows indicate particles that are only attached to cells and blue arrows indicate internalized particles; scale bar: 20 μm.

5 kV, Everhart-Thornley detector). Representative SEM pictures of cells with attached and internalized particles are presented in Fig. 1 (C and D).

2.3. Statistical analysis

Statistical analysis was conducted using R studio software (Version 1.0.143). The data of the individual cell experiments were tested for normal distribution (Shapiro-Wilk test) and homogeneity of variances (Levene test). For the adhesion force experiments using optical tweezers, the assumptions for an ANOVA with a Tukey post-hoc test were met, whereas for the particle-cell-interactions and number of internalized particles, a Kruskal-Wallis test with a Games Howell post hoc test (p-adjust method for multiple nesting: Bonferroni Holm) was conducted.

3. Results

First, we investigated whether the coating with an eco-corona from FW and SW and the opsonisation of the microplastic particles with IgG was successful using SEM. The images confirm the presence of an eco-corona on the microplastic particles surfaces, by showing deposits on their surfaces incubated in FW and SW (Fig. 2 A and B, respectively) that were absent on the microplastic particles incubated in UW (Fig. 2 C). Likewise, the IgG-coated carboxylated microplastic particles show a visibly covered surface, compared to the untreated carboxylated particles (Fig. 2 D and E, respectively), indicating a successful coating with IgG. Since antibodies such as IgG are proteins, the IgG particles served as reference particles for the eco-corona protein quantification. The protein content within an eco-corona is expected to be lower compared to a specific coating of microplastic particles with IgG, since an eco-corona can consist of other biomolecules, like lipids or carbohydrates. Using the total ion chromatograms, which represent the signal intensities of all peptide ions detected by the mass spectrometer, we observed on average a 2.8 × higher protein amount for the microplastic particles opsonized with IgG compared to the eco-corona microplastic particles (Fig. S1). The use of total ion current is a common approach in proteomics experiments [69].

Furthermore, we analysed the proteinaceous composition of the two eco-coronae formed in FW and SW and found that they are distinct from each other. None of the proteins found in an FW-derived eco-corona were present in an SW eco-corona and *vice versa* (results from the database searches are available in supplement table ST1). We unambiguously identified various peptides from bacterial and algal species. The most proteins were identified in the SW incubated samples (71 unique peptides for bacteria, 28 unique peptides for algae) which could be assigned to 19 bacterial proteins and 13 algae proteins, respectively. In the search against the algae database, nearly all identified proteins were annotated as "unnamed protein product" and therefore not assigned to specific protein classes. In addition, we identified several bacterial proteins from the genus *Marivita* in the SW samples. The genus

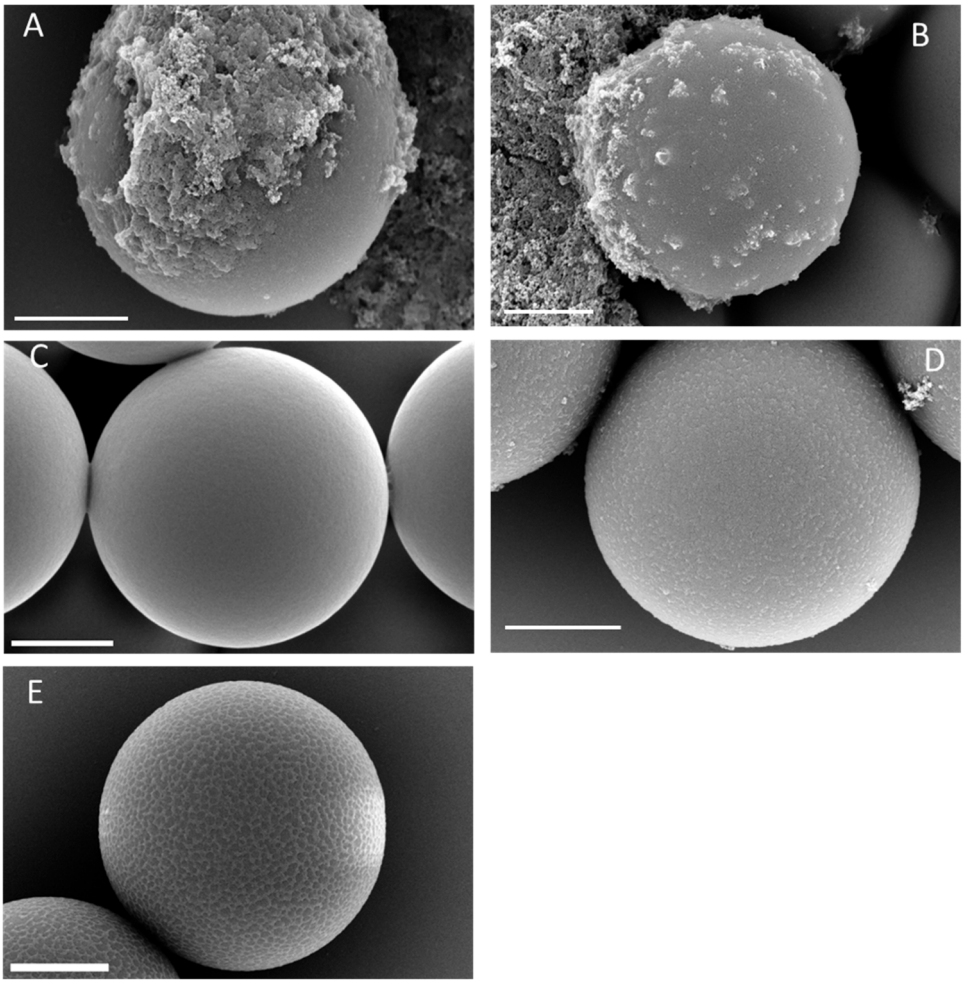

Fig. 2. Scanning electron microscopy images of 3 μm sized microplastic particles with different treatments. Microplastic particles coated with an eco-corona due to FW (A) or SW incubation (B) and particles without an eco-corona due to incubation in UW (C). COOH functionalized microplastic particles (D) were additionally opsonized with IgG (E). Both particles coated with an eco-corona show deposits on the initially smooth surface, the COOH functionalized microplastic particles show a rough surface which is coated by a net-like structure after the opsonization with IgG; scale bar: 1 μm.

Marivita belongs to the *Roseobacter* clade (within the *Rhodobacteraceae* family), which represent some of the most abundant organisms in the marine environment and is also known to play key roles in many marine biochemical processes [57–59]. However, it should be noted that although we have searched our mass spectrometry data against all known SW and FW protein sequences, many microorganisms have not yet been sequenced, so that an exact assignment of the taxa is not possible.

We then investigated, whether the differences in the proteinaceous composition of the different eco-coronae lead to differences in their interactions with cells. Therefore, we quantified the adhesion between microplastic particles and cells by using a microfluidic microscopy platform and optical tweezers. Both, the fraction of remaining particles (microfluidics results are presented in supplementary information, Fig. S2, S3, S4) and the adhesion forces measured with optical tweezers, which corresponds to the force needed to pull the microplastic particle away from the cell membrane, were higher for microplastic particles coated with an eco-corona (average adhesion forces: FW: 2.5 ± 0.5 pN and SW: 1.5 ± 0.2 pN) compared to the microplastic particles without an eco-corona (UW: 0.6 ± 0.1 pN, average loading rate: 50 pN/s) (Fig. 3). We did not observe a significant difference for the adhesion forces between microplastic particles coated with an eco-corona from

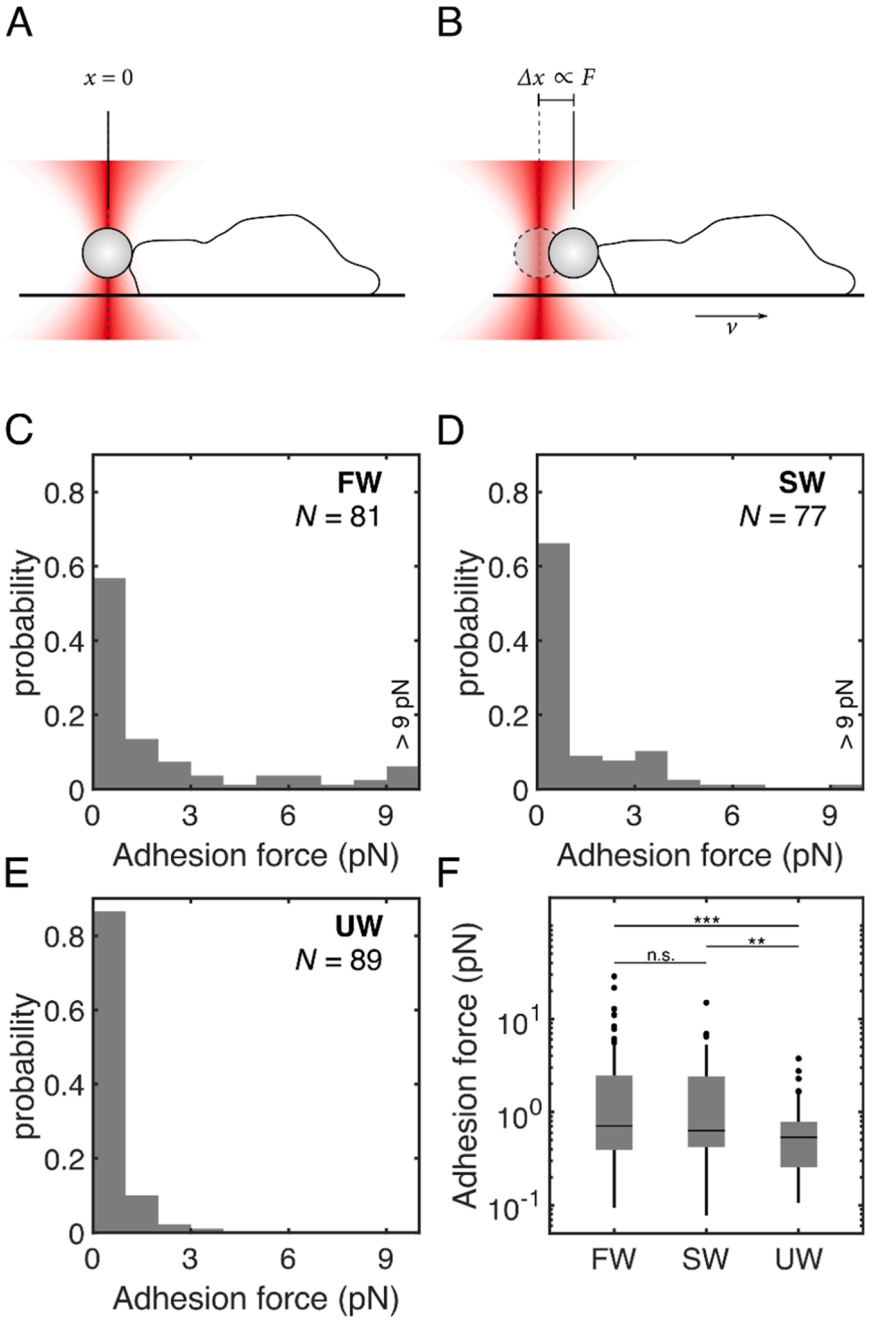

Fig. 3. Adhesion forces between microplastic particles and cells. To measure the adhesion forces between microplastic particles and cells, we used optical tweezers. A: After trapping a particle, we moved a cell close to the particle and made contact for 1 s. B: Then, the cell was moved away from the particle (average loading rate: 50 pN/s), and the displacement Δx of the particle from the trap center was measured to determine the adhesion force. C-E: Distribution of the adhesion force for FW, SW, and UW particles. F: The average adhesion force for FW (2.5 ± 0.5 pN) and SW (1.5 ± 0.2 pN) were significantly higher than the adhesion force of UW particles (0.6 ± 0.1 pN). However, there was no significant difference between FW and SW particles. (Kruskal-Wallis Test with Games-Howell post-hoc test: n.s.: two-sided $p > 0.05$, **: two-sided $p \leq 0.01$, ***: two-sided $p \leq 0.001$).

FW and SW. However, we show that the number of particle-cell-interactions significantly (*** = $p \leq 0.001$) differs between all microplastic particles, with a significantly higher number of particle-cell-interactions of microplastic particles coated with an eco-corona from FW compared to SW ($p \leq 0.001$, Fig. S5). The same pattern was observed for the internalization of all tested microplastic particles. The microplastic particles coated with an eco-corona significantly ($p \leq 0.001$) more often become internalized than microplastic particles without an eco-corona and significantly ($p \leq 0.001$) less than microplastic particles opsonized with IgG, with FW showing a significantly higher number of internalized microplastic particles compared to SW (*** = $p \leq 0.001$, Fig. S5).

Since we did find differences in the proteinaceous composition of the two eco-coronae and also significant differences for the particle-cell-interactions and internalization between FW and SW we investigated the underlying internalization mechanisms. The inhibition of the actin-based internalization mechanisms significantly ($p \leq 0.001$) reduced the internalization for all tested microplastic particles compared to their corresponding controls (Fig. 4). Interestingly, the inhibition of phagocytosis, did not significantly reduce the internalization of microplastic particles coated with an eco-corona from SW, but significantly (IgG and FW: $p \leq 0.001$; UW: $p \leq 0.01$) reduced the internalization of all other particle types compared to the corresponding controls.

4. Discussion

We show that the proteinaceous composition of the eco-corona on microplastic particles incubated either in FW or SW is distinct from each other. Although these differences in eco-corona composition did not lead to differences in the adhesion strength to cellular membranes, the number of particle-cell-interactions, internalized particles and their underlying internalization mechanisms significantly differ between the eco-coronae formed in different environments.

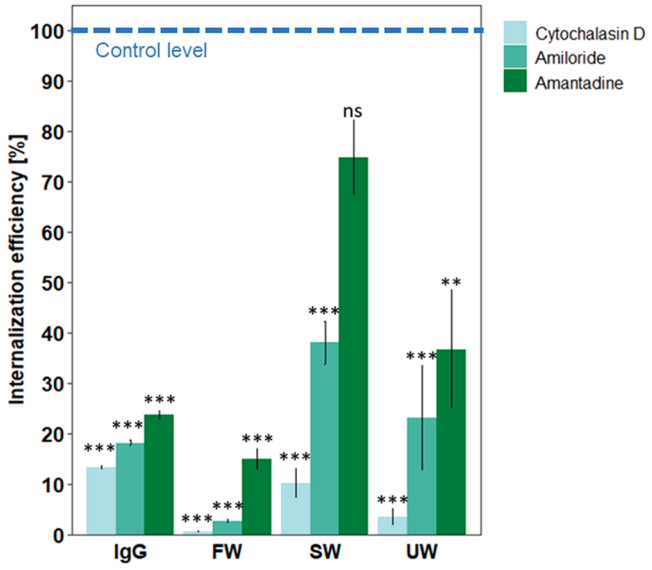

Fig. 4. Internalization efficiency after drug treatment compared to control (100 % = control). For each particle type a corresponding control without inhibiting the internalization mechanisms was conducted. IgG = Microplastic particles opsonized with immunoglobulin G (positive control), FW = Microplastic particles incubated for two weeks in freshwater, SW = Microplastic particles incubated for two weeks in saltwater and UW = Microplastic particles incubated for two weeks in ultrapure water (no eco-corona, negative control). Cytochalasin D and Amiloride significantly inhibited the internalization for all microplastic particle types compared to their corresponding controls (*** = $p \leq 0.001$). Amantadine significantly inhibited the internalization of IgG, FW (*** = $p \leq 0.001$) and UW (** = $p \leq 0.01$) but not for microplastic particles incubated in saltwater (ns= $p > 0.05$, all numbers indicate mean ± se).

When a particle encounters a cell, it can bind to the cellular membrane. This binding can depend on the biological identity, like the composition of surface coatings of a particle initiating specific receptor-mediated interactions or on the physicochemical properties of a particle initiating the interaction via unspecific electrostatic forces [14,17,20,60,61]. It has already been shown that the physicochemical properties of microplastic particles determine how they interact with cells. Generally it was described that the coating with an eco-corona makes the surface of a particle rougher [19] but softer [32], and surface functional groups are introduced [19,21] changing the microplastic particles' zeta potential [19]. These changes can lead to a higher interaction between microplastic particles and cells compared to their pristine counterparts [19,20]. Here we show that also the proteinaceous composition found on the surface of microplastic particles coated with eco-coronae formed under different environmental conditions are different. Although the quantity of proteins was higher in the SW compared to the FW eco-corona, the number of particle-cell interactions and the internalization was higher for microplastic particles coated with an eco-corona from FW. This finding suggests that the composition of the proteins within an eco-corona (and also other molecules) is more critical than the quantity of proteins. One type of protein may be more likely to interact with cell receptors than others, leading to differences in cellular internalization. Furthermore, it has been described that proteins can also bind to specific receptors, initiating a so-called "don't eat me signal", and inhibiting cellular internalization [75]. However, the "don't eat me" signal, initiated by the binding of CD47 to its receptor SIRPa [75] is highly specific, and it is unclear whether similar processes can occur for proteins within an eco-corona interacting cell membrane receptors.

Our results show that the physicochemical properties of microplastic particles are important for the particle-cell interaction, but the mechanisms involved in microplastic particle internalization might be driven by the particles' biological identity, e.g. the coating with proteins.

Macrophages represent the forefront of the innate immune defence against foreign particulate matter such as bacterial invaders [62]. The most prominent kinds of proteins we found in both eco-coronae are associated with prokaryotic cellular membranes (See table ST1). The proteins in the eco-corona may expose ligands resembling those of prokaryotes that can be recognized by membrane receptors facilitating particle internalization via phagocytosis [14]. The most relevant receptors to induce internalization are opsonic and non-opsonic receptors. Opsonic receptors are highly specific and bind to host-derived proteins, such as antibodies and complement components, initiating the process of phagocytosis. Non-opsonic receptors recognize pathogen-associated molecular patterns, e.g., from microorganisms or apoptotic cells [76]. Many membrane receptors have dual functions like the mediation of the particle attachment as well as the particle internalization. Those adhesion and internalization receptors can also activate and inhibit each other's functions [63–65]. Therefore, the proteinaceous components of the eco-corona may alter the particles' adhesion to cells, the number of particle-cell-interactions, as well as their internalization. By inhibiting phagocytosis with Amantadine we show that microplastic particles coated with an eco-corona derived from SW most likely become internalized accidentally via macropinocytosis, not phagocytosis. Interestingly, Deloid et al. [53] just recently described that PS nanoparticles without an eco-corona are actively internalized in an *in vitro* human small intestine model and not via macropinocytosis. This might be due to the small size of the PS nanoparticles (26 nm in diameter) and their pristine surface properties, since the internalization mechanism are different for nanoparticles compared to microparticles. In general, nanoparticles have additional internalization mechanisms compared to microparticles. The most often described internalization mechanisms for nanoparticles are clathrin-mediated endocytosis, caveolae-dependent endocytosis, clathrin/caveolae-independent endocytosis, and passive diffusion [77,78]. For particles larger than 0.5 μm phagocytosis and

macropinocytosis are the main internalization mechanisms [63]. Since we used microplastic particles of 3 μm in diameter, it is highly unlikely that other internalization processes than phagocytosis and macropinocytosis are responsible for the particle internalization. The introduction of an eco-corona on the surface of microplastic particles leads to a very small increase in the size of the particles. However this increase was described to be not significant compared to particles without an eco-corona [19].

Furthermore, as already described, macrophages are professional phagocytes compared to epithelial cells and therefore the internalization mechanisms, especially for microparticles can be different. Particulate internalization via macropinocytosis is not initiated by the direct interaction of ligands on the particle surface with cell membrane receptors but rather randomly [15,66]. Cells of the innate immune system constitutively perform membrane ruffling [16,67], making the internalization of microplastic particles that adhere to cellular membranes unspecifically via electrostatic forces more likely. Since microplastic particles coated with an eco-corona increase the number of particle-cell-interactions and stronger adhere to cellular membranes the accidentally occurring internalization via membrane ruffling can be enhanced. Additionally, growth factors that may be components of an eco-corona, increase membrane ruffling and, consequently, macropinocytosis [18,67].

One explanation that microplastic particles coated with an eco-corona from SW seem to mainly become internalized via macropinocytosis is the presence of salts within the eco-corona [21]. The salt concentration in the saltwater incubation media is 35 ‰; therefore, salts may also be present in the eco-corona. Interestingly extracellular calcium can drive constitutive macropinocytosis in human monocyte-derived macrophages [16]. Calcium is the fifth most abundant salt in our incubation medium (460 mg/L), suggesting that calcium is also present in the eco-corona, supporting the process of membrane ruffling. Thus, macropinocytosis might be the main internalization pathway for microplastic particles coated with an eco-corona from SW. For the other tested microplastic particle types, namely FW, IgG and UW, the internalization process are most probably a combination of both mechanisms, phagocytosis and macropinocytosis. Particles opsonized with IgG highly specifically bind to the opsonic Fcγ receptor, and therefore, their main internalization pathway is receptor-mediated phagocytosis [68,70]. The strong binding of IgG to Fcγ-receptors is also shown by the strong adhesion between the IgG-coated particles and cells (Fig. S2). Additionally, the adhesion forces of IgG microplastic particles were often higher than the maximal force that the optical trap could produce, and we could therefore not quantify the adhesion forces of IgG microplastic particles. Although not statistically significant, the adhesion forces of microplastic particles incubated in FW are higher than those incubated in SW. This might be due to the different protein composition on microplastic particles coated with an eco-corona from FW compared to SW. In general, the process of phagocytosis is not solely facilitated through opsonic receptors, such as the Fcγ receptor. Some non-opsonic receptors, like C-type lectins, lectin-like recognition molecules (e.g. CD33), and scavenger receptors [73,76], can initiate phagocytosis, whilst others, for example, toll-like receptors, can bind to pathogen-associated molecular patterns but do not initiate the process of phagocytosis. However, toll-like receptors can prime the cell for phagocytosis or cooperate with phagocytic receptors, enhancing the process of phagocytosis [76]. Non-opsonic receptors might therefore play an important role during recognition and internalization of FW and UW microplastic particles. However, this is speculative and needs further investigation.

UW microplastic particles only very occasionally bound to cellular membranes or became internalized. However, the small number of particles interacting with cells and becoming internalized may occur for different reasons. Since LC-MS/MS is a highly sensitive technique, we also found proteins on the microplastic particles incubated in UW, such as human keratin, which is a common contamination in all types of plastics [71]. Furthermore, we identified the bacterial protein "chaperonin GroEL", from different bacterial taxa, in the FW, SW, and UW samples, which was absent in IgG. In FW and UW, GroEL from the genus *Ralstonia* was identified. *Ralstonia* is known to be a common contaminant in laboratory kits or reagents (e.g. DNA extraction kits) [72], and does therefore likely not originate from the eco-corona. The proteins detected on the particles without an eco-corona originating from contamination may already be sufficient to cause weak adhesion and a small number of internalizations. Furthermore, although the particles were added to the experimental setup in a pristine form without an eco-corona, proteins and other biomolecules from the surrounding cell culture media can adsorb to the surface of the particles [19,24,61] without an eco-corona explaining the small number of interactions.

The internalization of microplastic particles coated with an eco-corona either via phagocytosis or macropinocytosis may have severe effects on the cells. In the case of phagocytosis, the presence of the receptor on the plasma membrane works as a sensor for detecting external signals, e.g. the binding of a microplastic particle coated with an eco-corona to the cell membrane which leads to the transmission of signaling cascade responses for the extracellular to intracellular environment of cells. The overstimulation of cells by encountering microplastic particles from the environment may encounter a higher risk of alteration and dysfunction of phagocytosis, which consequently can promote several chronic diseases, including cancer, neurological disorders such as Alzheimer's disease, Parkinson's disease, and amyotrophic lateral sclerosis, cardiovascular disease, and inflammatory bowel disease [73]. In the case of macropinocytosis, the higher likeliness of microplastic particles from the environment interacting with macrophages can also lead to the release of cytokines, such as growth factors, that can eventually enhance the process of macropinocytosis. This overstimulation can lead to a dysregulation of the macropinocytosis pathway, further corroborating many physiological and pathological consequences, including dysregulated immune response, dysbiosis, and chronic human diseases. Therefore, in-depth scientific validations related to mechanisms and targets of endocytosis pathways may provide a better understanding of diagnosing and treating diseases [53,73,74].

5. Conclusions

We showed that the proteinaceous composition of the eco-corona differs between microplastic particles that were incubated in FW and SW. These differences did not significantly change the adhesion of the particles to the cells but it affected the number of particle-cell-interactions and their cellular internalization. We found that microplastic particles coated with an eco-corona from SW mainly become internalized via macropinocytosis, whereas the other particle types seem to be internalized via macropinocytosis and phagocytosis. As the molecular signaling cascades involved in different internalization pathways play an important role in determining the cellular fate of internalized microplastic particles, environmental microplastic particles might cause different cellular reactions depending on their eco-corona composition. Such cellular reactions are the basis for potentially adverse effects of environmental microplastic particles on cells, tissues, and consequently organisms. Therefore, our results may help to better understand the hazard potential associated with microplastic particles in the environment.

Environmental implication

Harmful effects of microplastics (MPs) on organisms were shown, especially related to their ingestion or inhalation. Upon uptake the MPs can translocate from the exposed organs into other tissues via cellular internalization. The cellular internalization of MPs was shown to be enhanced for environmentally exposed MPs, coated with an eco-corona. We show that the composition of the eco-corona formed in different environments leads to different internalization pathways. To be able to

understand the adverse effects of MPs from the environment on organisms and human health a mechanistic understanding of their interactions with cells is essential.

Funding

This work was supported by the Deutsche Forschungsgemeinschaft (DFG, German Research Foundation) – project number 391977956-SFB 1357; and the European Union's Horizon2020 Research and Innovation programme, under the Grant Agreement number 965367 (PlasticsFatE). The SEM was funded by the Deutsche Forschungsgemeinschaft (DFG GZ: INST 91/366-1 FUGG and INST 91/427-1 FUGG). AFRMR was supported by a scholarship of the elite network of Bavaria (BayEFG). S.W. was supported by the elite network of Bavaria (Study Program Biological Physics). S.W. and AFRM.R. were supported by the University of Bayreuth Graduate School.

CRediT authorship contribution statement

Laforsch Christian: Writing – review & editing, Writing – original draft, Validation, Supervision, Software, Resources, Project administration, Methodology, Investigation, Funding acquisition, Conceptualization. **Kress Holger:** Writing – review & editing, Writing – original draft, Validation, Supervision, Software, Resources, Project administration, Methodology, Investigation, Funding acquisition, Conceptualization. **Fröhlich Thomas:** Writing – review & editing, Writing – original draft, Supervision, Software, Resources, Methodology, Investigation, Funding acquisition, Formal analysis, Data curation. **Wilde Magdalena V.:** Writing – review & editing, Writing – original draft, Visualization, Validation, Methodology, Formal analysis, Data curation. **Wieland Simon:** Writing – review & editing, Writing – original draft, Visualization, Validation, Methodology, Investigation, Formal analysis, Data curation, Conceptualization. **Ramsperger Anja F.R.M:** Writing – original draft, Visualization, Validation, Methodology, Investigation, Formal analysis, Data curation, Conceptualization.

Declaration of Competing Interest

The authors declare that they have no known competing financial interests or personal relationships that could have appeared to influence the work reported in this paper.

Acknowledgments

We thank the technicians Mechthild Kredler, Ursula Wilczek, Marion Preiß, Heghnar Martirosyan, Hannah Ganzleben, Isabell Stahlmann, Andrea Hanold, Kathrin Weidner-Hertrampf and Daniela Grätz from the Department of Animal Ecology I and the Biological Physics Group of the University of Bayreuth and Miwako Kösters from the Ludwig Maximilian University of Munich.

Author contributions

AFRMR, CL and HK initiated the research. All authors planned the research. AFRMR and SW performed the microplastic particle incubation experiments. AFRMR and SW prepared the SEM samples and SW imaged the SEM samples. AFRMR performed the cell experiments regarding particle-cell interactions, internalization and inhibition of internalization mechanisms. SW performed the particle adhesion experiments. MVW performed LC-MS/MS experiments and data evaluation. AFRMR, SW and MVW wrote the first draft of the manuscript. AFRMR, SW, MVW, TF, HK and CL reviewed and edited the manuscript

Appendix A. Supporting information

Supplementary data associated with this article can be found in the online version at doi:10.1016/j.jhazmat.2025.137647.

Data availability

Data will be made available on request.

References

[1] Hartmann, N.B., Hüffer, T., Thompson, R.C., Hassellöv, M., Verschoor, A., Daugaard, A.E., Rist, S., Karlsson, T., Brennholt, N., Cole, M., et al., 2019. Are we speaking the same language? Recommendations for a definition and categorization framework for plastic debris. Environ Sci Technol 53, 1039–1047. https://doi.org/10.1021/acs.est.8b05297.

[2] MacLeod, M., Arp, H.P.H., Tekman, M.B., Jahnke, A., 2021. The global threat from plastic pollution. Science 373, 61–65. https://doi.org/10.1126/science.abg5433.

[3] Imhof, H.K., Ivleva, N.P., Schmid, J., Niessner, R., Laforsch, C., 2013. Contamination of beach sediments of a subalpine lake with microplastic particles. Curr Biol 23, R867–R868. https://doi.org/10.1016/j.cub.2013.09.001.

[4] Gilfedder, B.S., Elagami, H., Boos, J.P., Brehm, J., Schott, M., Witt, L., Laforsch, C., Frei, S., 2023. Filter feeders are key to small microplastic residence times in stratified lakes: a virtual experiment. Sci Total Environ 890, 164293. https://doi.org/10.1016/j.scitotenv.2023.164293.

[5] Jemec, A., Horvat, P., Kunej, U., Bele, M., Kržan, A., 2016. Uptake and effects of microplastic textile fibers on freshwater crustacean daphnia magna. Environ Pollut 219, 201–209. https://doi.org/10.1016/j.envpol.2016.10.037.

[6] von Moos, N., Burkhardt-Holm, P., Koehler, A., 2012. Uptake and effects of microplastics on cells and tissue of the blue mussel mytilus edulis l. after an experimental exposure. Environ Sci Technol 46, 327–335. https://doi.org/10.1021/es302332w.

[7] Brehm, J., Wilde, M.V., Reiche, L., Leitner, L.C., Petran, B., Meinhart, M., Wieland, S., Ritschar, S., Schott, M., Boos, J.P., et al., 2022. In-depth characterization revealed polymer type and chemical content specific effects of microplastic on dreissena bugensis. J Hazard Mater 437. https://doi.org/10.1016/j.jhazmat.2022.129351.

[8] Kahane-Rapport, S.R., Czapanskiy, M.F., Fahlbusch, J.A., Friedlaender, A.S., Calambokidis, J., Hazen, E.L., Goldbogen, J.A., Savoca, M.S., 2022. Field measurements reveal exposure risk to microplastic ingestion by filter-feeding megafauna. Nat Commun 13, 6327. https://doi.org/10.1038/s41467-022-33334-5.

[9] Wieland, S., Balmes, A., Bender, J., Kitzinger, J., Meyer, F., Ramsperger, A.F., Roeder, F., Tengelmann, C., Wimmer, B.H., Laforsch, C., et al., 2022. From properties to toxicity: comparing microplastics to other airborne microparticles. J Hazard Mater 428, 128151. https://doi.org/10.1016/j.jhazmat.2021.128151.

[10] Ramsperger, A.F.R.M., Bergamaschi, E., Panizzolo, M., Fenoglio, I., Barbero, F., Peters, R., Undas, A., Purker, S., Giese, B., Lalyer, C.R., et al., 2023. Nano- and microplastics: a comprehensive review on their exposure routes, translocation, and fate in humans. NanoImpact 29. https://doi.org/10.1016/j.impact.2022.100441.

[11] Wright, S.L., Kelly, F.J., 2017. Plastic and human health: a micro issue? Environ Sci Technol 51, 6634–6647. https://doi.org/10.1021/acs.est.7b00423.

[12] Rohrbach, A., Meyer, T., Stelzer, E.H.K., Kress, H., 2020. Measuring stepwise binding of thermally fluctuating particles to cell membranes without fluorescence. Biophys J 118, 1850–1860. https://doi.org/10.1016/j.bpj.2020.03.005.

[13] Freeman, S.A., Grinstein, S., 2014. Phagocytosis. Macrophages Biol Role Pathol Dis 91, 109. https://doi.org/10.1007/978-1-4939-1311-4_5.

[14] Forest, V., Cottier, M., Pourchez, J., 2015. Electrostatic interactions favor the binding of positive nanoparticles on cells: a reductive theory. Nano Today 10, 677–680. https://doi.org/10.1016/j.nantod.2015.07.002.

[15] Mylvaganam, S., Freeman, S.A., Grinstein, S., 2021. The cytoskeleton in phagocytosis and macropinocytosis. Curr Biol 31, R619–R632. https://doi.org/10.1016/j.cub.2021.01.036.

[16] Canton, J., 2018. Macropinocytosis: new insights into its underappreciated role in innate immune cell surveillance. Front Immunol 9, 1–8. https://doi.org/10.3389/fimmu.2018.02286.

[17] Swanson, J.A., 2008. Shaping cups into phagosomes and macropinosomes. Nat Rev Mol Cell Biol 9, 639–649. https://doi.org/10.1038/nrm2447.

[18] Griffiths, G., Gruenberg, J., Marsh, M., Wohlmann, J., Jones, A.T., Parton, R.G., 2022. Nanoparticle entry into cells; the cell biology weak link. Adv Drug Deliv Rev 188, 114403. https://doi.org/10.1016/j.addr.2022.114403.

[19] Wieland, S., Ramsperger, A.F.R.M., Gross, W., Lehmann, M., Witzmann, T., Caspari, A., Obst, M., Gekle, S., Auernhammer, G.K., Fery, A., et al., 2024. Nominally identical microplastic models differ greatly in their particle-cell interactions. Nat Commun 15, 1–17. https://doi.org/10.1038/s41467-024-45281-4.

[20] Ramsperger, A.F.R.M., Jasinski, J., Völkl, M., Witzmann, T., Meinhart, M., Jérôme, V., Kretschmer, W.P., Freitag, R., Senker, J., Fery, A., et al., 2021. Supposedly identical microplastic particles substantially differ in their material properties influencing particle-cell interactions and cellular responses. J Hazard Mater 425, 127961. https://doi.org/10.1016/j.jhazmat.2021.127961.

[21] Ramsperger, A.F.R.M., Narayana, V.K.B., Gross, W., Mohanraj, J., Thelakkat, M., Greiner, A., Schmalz, H., Kress, H., Laforsch, C., 2020. Environmental exposure enhances the internalization of microplastic particles into cells. Sci Adv 6, 1–10. https://doi.org/10.1126/sciadv.abd1211.

[22] Rozman, U., Kalčíková, G., 2022. Seeking for a perfect (non-spherical) microplastic particle – the most comprehensive review on microplastic laboratory research. J Hazard Mater 424, 127529. https://doi.org/10.1016/j.jhazmat.2021.127529.

[23] Lundqvist, M., Stigler, J., Elia, G., Lynch, I., Cedervall, T., Dawson, K.A., 2008. Nanoparticle size and surface properties determine the protein corona with possible implications for biological impacts. Proc Natl Acad Sci 105, 14265–14270. https://doi.org/10.1073/pnas.0805135105.

[24] Lundqvist, M., Stigler, J., Cedervall, T., Berggård, T., Flanagan, M.B., Lynch, I., Elia, G., Dawson, K., 2011. The evolution of the protein corona around nanoparticles: a test study. ACS Nano 5, 7503–7509. https://doi.org/10.1021/nn202458g.

[25] Tenzer, S., Docter, D., Rosfa, S., Wlodarski, A., Rekik, A., Knauer, S.K., Bantz, C., Nawroth, T., Bier, C., Sirirattanapan, J., et al., 2011. Nanoparticle size is a critical physico- chemical determinant of the humanblood plasma corona: a comprehensive quantitative proteomic analysis. ACS Nano 5, 7155–7167. https://doi.org/10.1021/nn201950e.

[26] Tenzer, S., Docter, D., Kuharev, J., Musyanovych, A., Fetz, V., Hecht, R., Schlenk, F., Fischer, D., Kiouptsi, K., Reinhardt, C., et al., 2013. Rapid formation of plasma protein corona critically affects nanoparticle pathophysiology. Nat Nanotechnol 8, 772–781. https://doi.org/10.1038/nnano.2013.181.

[27] Fadare, O.O., Wan, B., Liu, K., Yang, Y., Zhao, L., Guo, L.H., 2020. Eco-corona vs protein corona: effects of humic substances on corona formation and nanoplastic particle toxicity in daphnia magna. Environ Sci Technol 54, 8001–8009. https://doi.org/10.1021/acs.est.0c00615.

[28] Brash, J.L., Horbett, T.A., 1995. Proteins at interfaces. Adv Protein Chem 32, 283–326. https://doi.org/10.1016/S0065-3233(08)60577-X.

[29] Nasser, F., Lynch, I., 2016. Secreted protein eco-corona mediates uptake and impacts of polystyrene nanoparticles on daphnia magna. J Proteom 137, 45–51. https://doi.org/10.1016/j.jprot.2015.09.005.

[30] Hlady, V.V., Buijs, J., 1996. Protein adsorption on solid surfaces. Curr Opin Biotechnol 7, 72–77. https://doi.org/10.1016/s0958-1669(96)80098-x.

[31] Monopoli, M.P., Åberg, C., Salvati, A., Dawson, K.A., 2012. Biomolecular coronas provide the biological identity of nanosized materials. Nat Nanotechnol 7, 779–786. https://doi.org/10.1038/nnano.2012.207.

[32] Witzmann, T., Ramsperger, A.F.R.M., Wieland, S., Laforsch, C., Kress, H., Fery, A., Auernhammer, G.K., 2022. Repulsive interactions of eco-corona-covered microplastic particles quantitatively follow modeling of polymer brushes. Langmuir 38, 8748–8756. https://doi.org/10.1021/acs.langmuir.1c03204.

[33] Nasser, F., Constantinou, J., Lynch, I., 2019. Nanomaterials in the environment acquire an “eco-corona” impacting their toxicity to daphnia magna—a call for updating toxicity testing policies. Proteomics 1–15. https://doi.org/10.1002/pmic.201800412.

[34] Keller, S., Berghoff, K., Kress, H., 2017. Phagosomal transport depends strongly on phagosome size. Sci Rep 1–15. https://doi.org/10.1038/s41598-017-17183-7.

[35] Cooksey, K.E., and Wigglesworth-Cooksey, B. (1995). Adhesion of bacteria and diatoms to surfaces in the sea: A review, https://doi.org/10.3354/ame009087 https://doi.org/10.3354/ame009087.

[36] Berghoff, K., Gross, W., Eisentraut, M., Kress, H., 2021. Using blinking optical tweezers to study cell rheology during initial cell-particle contact. Biophys J 120, 3527–3537. https://doi.org/10.1016/j.bpj.2021.04.034.

[37] Loeb, G., Neihof, R., 1975. Marine conditioning films. Adv Chem 145, 319–335. https://doi.org/10.1021/ba-1975-0145.

[38] Eisentraut, M., Sabri, A., Kress, H., 2023. The spatial resolution limit of phagocytosis. Biophys J 122, 868–879. https://doi.org/10.1016/j.bpj.2023.01.030.

[39] Lorite, G.S., Rodrigues, C.M., de Souza, A.A., Kranz, C., Mizaikoff, B., Cotta, M.A., 2011. The role of conditioning film formation and surface chemical changes on Xylella fastidiosa adhesion and biofilm evolution. J Colloid Interface Sci 359, 289–295. https://doi.org/10.1016/j.jcis.2011.03.066.

[40] Laforsch, C., Tollrian, R., 2000. A new preparation technique of daphnids for scanning electron microscopy using hexamethyldisilazane. Arch Fur Hydrobiol 149, 587–596. https://doi.org/10.1127/archiv-hydrobiol/149/2000/587.

[41] Rummel, C.D., Jahnke, A., Gorokhova, E., K?hnel, D., Schmitt-Jansen, M., 2017. The impacts of biofilm formation on the fate and potential effects of microplastic in the aquatic environment. Environ Sci Technol Lett. https://doi.org/10.1021/acs.estlett.7b00164.

[42] Perkins, D.N., Pappin, D.J., Creasy, D.M., Cottrell, J.S., 1999. Probability-based protein identification by searching sequence databases using mass spectrometry data. Electrophoresis 20, 3551–3567. https://doi.org/10.1002/(SICI)1522-2683(19991201)20:18< 3551::AID-ELPS3551> 3.0.CO;2-2.

[43] Wheeler, K.E., Chetwynd, A.J., Fahy, K.M., Hong, B.S., Tochihuitl, J.A., Foster, L.A., Lynch, I., 2021. Environmental dimensions of the protein corona. Nat Nanotechnol 16, 617–629. https://doi.org/10.1038/s41565-021-00924-1.

[44] Ishihama, Y., Oda, Y., Tabata, T., Sato, T., Nagasu, T., Rappsilber, J., Mann, M., 2005. Exponentially modified protein abundance index (emPAI) for estimation of absolute protein amount in proteomics by the number of sequenced peptides per protein. Mol Cell Proteom 4, 1265–1272. https://doi.org/10.1074/mcp.M500061-MCP200.

[45] Galloway, T.S., Cole, M., Lewis, C., 2017. Interactions of microplastic debris throughout the marine ecosystem. Nat Ecol Evol 1, 0116. https://doi.org/10.1038/s41559-017-0116.

[46] Perez-Riverol, Y., Csordas, A., Bai, J., Bernal-Llinares, M., Hewapathirana, S., Kundu, D.J., Inuganti, A., Griss, J., Mayer, G., Eisenacher, M., et al., 2019. The pride database and related tools and resources in 2019: improving support for quantification data. Nucleic Acids Res 47, D442–D450. https://doi.org/10.1093/nar/gky1106.

[47] Pulido-Reyes, G., Leganes, F., Fernández-Piñas, F., Rosal, R., 2017. Bio-nano interface and environment: a critical review. Environ Toxicol Chem 36, 3181–3193. https://doi.org/10.1002/etc.3924.

[48] Hendricks, A.G., Goldman, Y.E., 2017. In: Gennerich, A. (Ed.), Measuring Molecular Forces Using Calibrated Optical Tweezers in Living Cells Bt - Optical Tweezers: Methods and Protocols. Springer New York, pp. 537–552. https://doi.org/10.1007/978-1-4939-6421-5_21.

[49] Lewis, J.P., 1995. Template matching by cross correlation 2 normalized cross correlation. Can Image Process Pattern Recognit Soc 120–123.

[50] Koivusalo, M., Welch, C., Hayashi, H., Scott, C.C., Kim, M., Alexander, T., Touret, N., Hahn, K.M., Grinstein, S., 2010. Amiloride inhibits macropinocytosis by lowering submembranous pH and preventing Rac1 and Cdc42 signaling. J Cell Biol 188, 547–563. https://doi.org/10.1083/jcb.200908086.

[51] Gould, N.S., Min, E., Day, B.J., 2011. Macropinocytosis of extracellular glutathione ameliorates tumor necrosis factor α release in activated macrophages. PLoS One 6. https://doi.org/10.1371/journal.pone.0025704.

[52] Mahmoudi, M., Landry, M.P., Moore, A., Coreas, R., 2023. The protein corona from nanomedicine to environmental science. Nat Rev Mater 8, 422–438. https://doi.org/10.1038/s41578-023-00552-2.

[53] DeLoid, G.M., Yang, Z., Bazina, L., Kharaghani, D., Sadrieh, F., Demokritou, P., 2024. Mechanisms of ingested polystyrene micro-nanoplastics (MNPs) uptake and translocation in an in vitro tri-culture small intestinal epithelium. J Hazard Mater 473, 134706. https://doi.org/10.1016/j.jhazmat.2024.134706.

[54] Garcia Gil, M., Sanchez Crespo, M., 1983. Dansylcadaverine and rimantadine inhibition of phagocytosis, PAF-acether release, and phosphatidylcholine synthesis in human polymorphonuclear leukocytes. Immunopharmacology 6, 317–325. https://doi.org/10.1016/0162-3109(83)90037-1.

[55] Schlegel, R., Dickson, R.B., Willingham, M.C., Pastan, I.H., 1982. Amantadine and dansylcadaverine inhibit vesicular stomatitis virus uptake and receptor-mediated endocytosis of α2-macroglobulin. Proc Natl Acad Sci USA 79, 2291–2295. https://doi.org/10.1073/pnas.79.7.2291.

[56] Jonkman, J.E.N., Swoger, J., Kress, H., Rohrbach, A., Stelzer, E.H.K., 2003. Resolution in optical microscopy. Methods Enzym 360, 416–446. https://doi.org/10.1016/S0076-6879(03)60122-9.

[57] Pujalte, M.J., Lucena, T., Ruvira, M.A., Arahal, D.R., Macián, M.C., 2014. In: Rosenberg, E., DeLong, E.F., Lory, S., Stackebrandt, E., Thompson, F. (Eds.), The Family Rhodobacteraceae BT - The Prokaryotes: Alphaproteobacteria and Betaproteobacteria. Springer Berlin Heidelberg, pp. 439–512. https://doi.org/10.1007/978-3-642-30197-1_377.

[58] R. Budinoff, C., R. Dunlap, J., Hadden, M., and Buchan, A. (2011). <I>Marivita roseacus < /I>sp. nov., of the family <I>Rhodobacteraceae< /I> , isolated from a temperate estuary and an emended description of the genus <I>Marivita< /I> . J. Gen. Appl. Microbiol. *57*, 259–267. https://doi.org/10.2323/jgam.57.259.

[59] Bentzon-Tilia, M., Gram, L., 2017. In: Paterson, R., Lima, N. (Eds.), Biotechnological Applications of the Roseobacter Clade BT - Bioprospecting: Success, Potential and Constraints. Springer International Publishing, pp. 137–166. https://doi.org/10.1007/978-3-319-47935-4_7.

[60] Underhill, D.M., Goodridge, H.S., 2012. Information processing during phagocytosis. Nat Rev Immunol 12, 492–502. https://doi.org/10.1038/nri3244.

[61] Werner, M., Auth, T., Beales, P.A., Fleury, J.B., Höök, F., Kress, H., Van Lehn, R.C., Müller, M., Petrov, E.P., Sarkisov, L., et al., 2018. Nanomaterial interactions with biomembranes: bridging the gap between soft matter models and biological context. Biointerphases 13, 28501. https://doi.org/10.1116/1.5022145.

[62] Weiss, G., Schaible, U.E., 2015. Macrophage defense mechanisms against intracellular bacteria. Immunol Rev 264, 182–203. https://doi.org/10.1111/imr.12266.

[63] Aderem, a, Underhill, D.M., 1999. Mechanisms of phagocytosis in macrophages. Annu Rev Immunol 17, 593–623. https://doi.org/10.1146/annurev.immunol.17.1.593.

[64] Thomas, J.R., Paul, N.R., Morgan, M.R., 2019. Adhesion and growth factor receptor crosstalk mechanisms controlling cell migration. Essays Biochem 63, 553–567. https://doi.org/10.1042/EBC20190025.

[65] Monnet, C., Jacque, E., de Romeuf, C., Fontayne, A., Abache, T., Fournier, N., Dupont, G., Derache, D., Engrand, A., Bauduin, A., et al., 2021. The dual targeting of fcrn and fcγrs via monomeric Fc fragments results in strong inhibition of IgG-dependent autoimmune pathologies. Front Immunol 12, 1–18. https://doi.org/10.3389/fimmu.2021.728322.

[66] Kerr, M.C., Teasdale, R.D., 2009. Defining macropinocytosis. Traffic 10, 364–371. https://doi.org/10.1111/j.1600-0854.2009.00878.x.

[67] Swanson, J., Watts, C., 1995. Macropinocytosis. Trends Cell Biol 5, 424–428 https://doi.org/0.1016/s0962-8924(00)89101-1.

[68] Nimmerjahn, F., Ravetch, J.V., 2008. Fcγ receptors as regulators of immune responses. Nat Rev Immunol 8, 34–47. https://doi.org/10.1038/nri2206.

[69] Zauber, H., Schüler, V., Schulze, W., 2013. Systematic evaluation of reference protein normalization in proteomic experiments. Front Plant Sci 4, 25. https://doi.org/10.3389/fpls.2013.00025.

[70] Bournazos, S., Gupta, A., Ravetch, J.V., 2020. The role of IgG Fc receptors in antibody-dependent enhancement. Nat Rev Immunol 20, 633–643. https://doi.org/10.1038/s41577-020-00410-0.

[71] Frankenfield, A.M., Ni, J., Ahmed, M., Hao, L., 2022. Protein contaminants matter: building universal protein contaminant libraries for DDA and DIA proteomics. J Proteome Res 21, 2104–2113. https://doi.org/10.1021/acs.jproteome.2c00145.

[72] Salter, S.J., Cox, M.J., Turek, E.M., Calus, S.T., Cookson, W.O., Moffatt, M.F., Turner, P., Parkhill, J., Loman, N.J., Walker, A.W., 2014. Reagent and laboratory contamination can critically impact sequence-based microbiome analyses. BMC Biol 12, 87. https://doi.org/10.1186/s12915-014-0087-z.

[73] Pathak, C., Vaidya, F.U., Waghela, B.N., Jaiswara, P.K., Gupta, V.K., Kumar, A., Rajendran, B.K., Ranjan, K., 2023. Insights of endocytosis signaling in health and disease. Int J Mol Sci 24. https://doi.org/10.3390/ijms24032971.
[74] Adler, M.Y., Issoual, I., Rückert, M., Deloch, L., Meier, C., Tschernig, T., Alexiou, C., Pfister, F., Ramsperger, A.F.R.M., Laforsch, C., et al., 2024. Effect of micro- and nanoplastic particles on human macrophages. J Hazard Mater 471, 134253. https://doi.org/10.1016/j.jhazmat.2024.134253.
[75] Fehervari, Z., 2015. Don't eat me, activate me. Nat Immunol 16, 1113. https://doi.org/10.1038/ni.3303.
[76] Uribe-Querol, E., Rosales, C., 2020. Phagocytosis: our current understanding of a universal biological process. Front Immunol 11. https://doi.org/10.3389/fimmu.2020.01066.
[77] Behzadi, S., Serpooshan, V., Tao, W., Hamaly, M.A., Alkawareek, M.Y., Dreaden, E. C., Brown, D., Alkilany, A.M., Farokhzad, O.C., Mahmoudi, M., 2017. Cellular uptake of nanoparticles: journey inside the cell. Chem Soc Rev 46, 4218–4244. https://doi.org/10.1039/c6cs00636a.
[78] Rennick, J.J., Johnston, A.P.R., Parton, R.G., 2021. Key principles and methods for studying the endocytosis of biological and nanoparticle therapeutics. Nat Nanotechnol 16, 266–276. https://doi.org/10.1038/s41565-021-00858-8.